Supporting Information

A unified electrocatalytic platform for the chemicals-H_2-electricity triad from biomass via interfacial electronic engineering

Wei Wang[1], Xiaoyang He[1], Shuai Dong[1], Jianying Wang[1], Deli Wu[2], Zuofeng Chen[1,*]

[1]School of Chemical Science and Engineering, Tongji University, 1239 Siping Road, Shanghai 200092, China;

[2]State Key Laboratory of Pollution Control and Resources Reuse, College of Environmental Science & Engineering, Tongji University, 1239 Siping Road, Shanghai 200092, China.

E-mail: zfchen@tongji.edu.cn (Z. F. Chen)

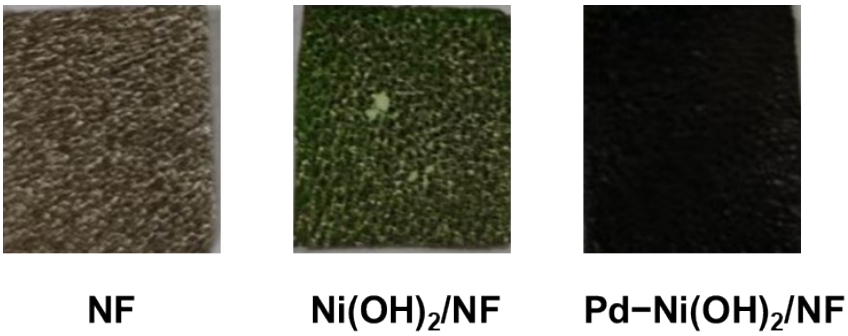

Figure S1. Optical photographs of the pristine NF, $Ni(OH)_2$/NF and Pd−$Ni(OH)_2$/NF.

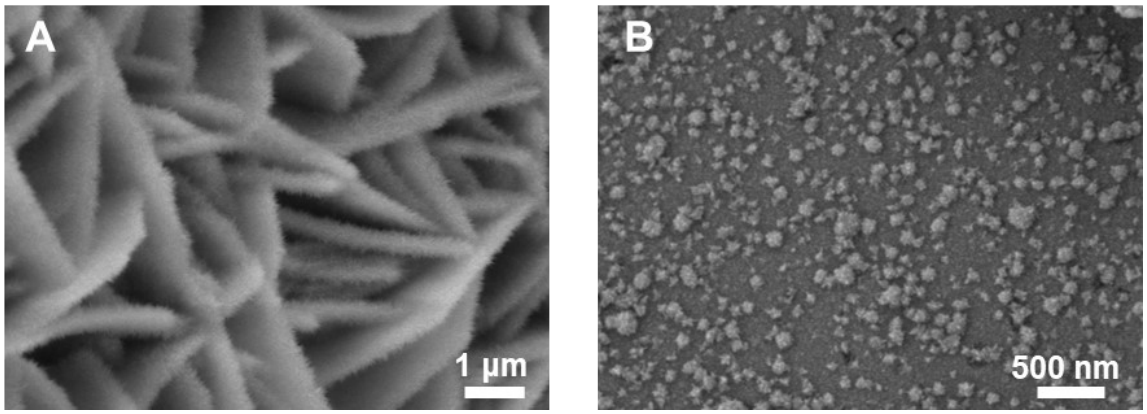

Figure S2. SEM images of the as-prepared (A) $Ni(OH)_2$/NF and (B) Pd/NF.

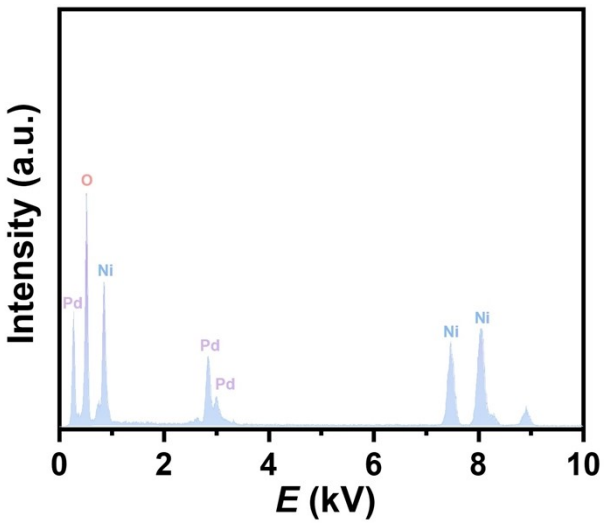

Figure S3. TEM-EDS of the nanosheet material scrapped from Pd−$Ni(OH)_2$/NF electrode.

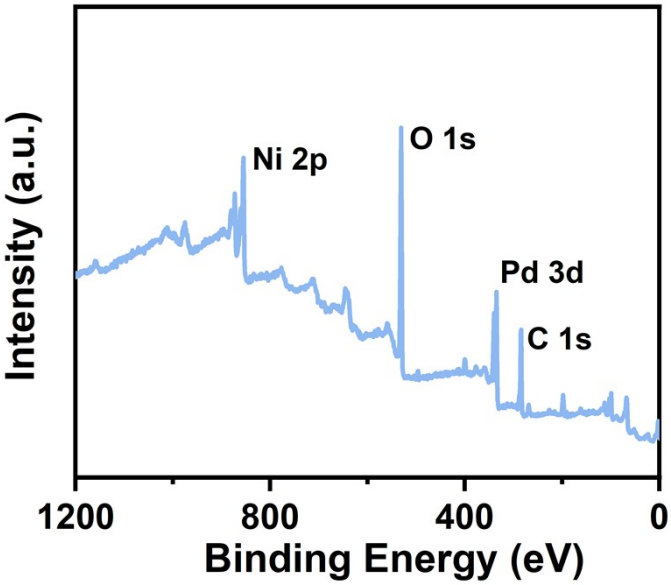

Figure S4. Survey XPS spectrum of the Pd−$Ni(OH)_2$/NF.

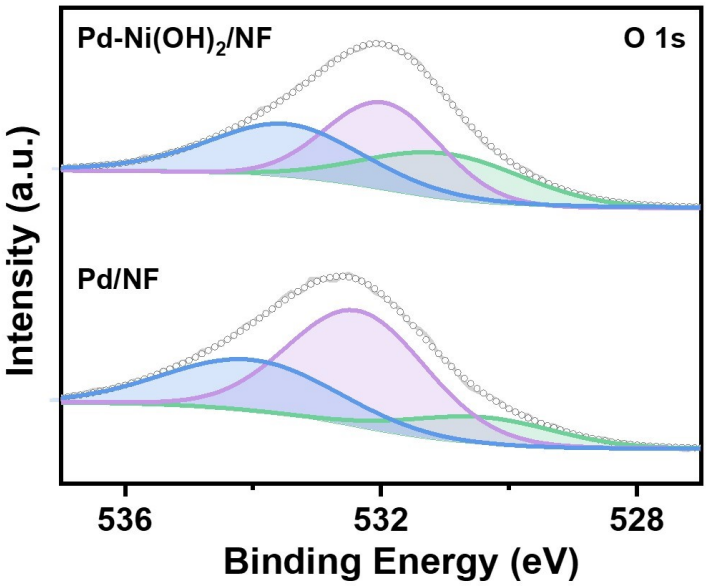

Figure S5. XPS spectra of O 1s on the different electrodes.

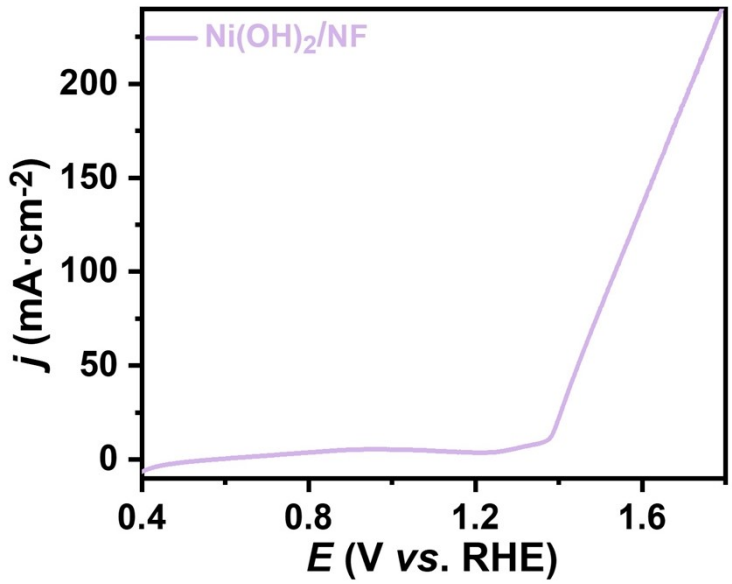

Figure S6. LSV curve of $Ni(OH)_2$/NF electrode in 1 M KOH with 0.1 M 1,3-PDO.

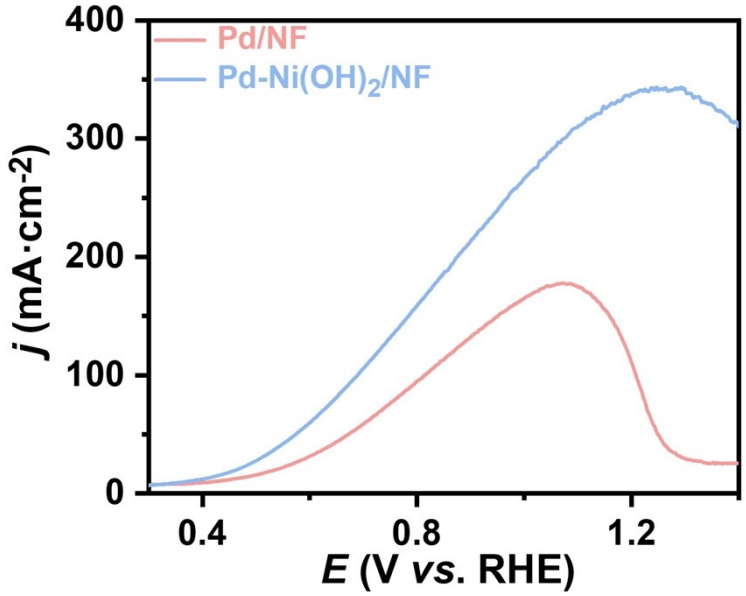

Figure S7. LSV curves of Pd−$Ni(OH)_2$/NF and Pd/NF electrodes in 1 M KOH with 0.1 M 1,3-PDO.

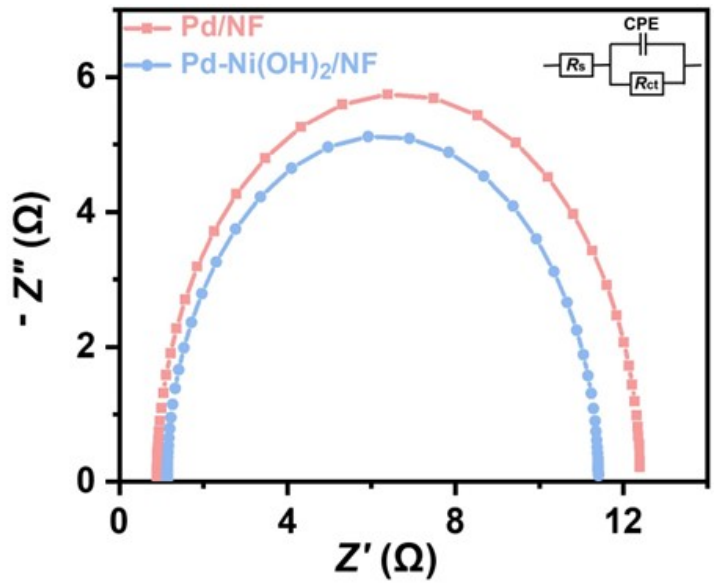

Figure S8. Nyquist plots of Pd−$Ni(OH)_2$/NF and Pd/NF electrodes at 0.5 V (vs. RHE) in 1 M KOH solution with 0.1 M 1,3-PDO.

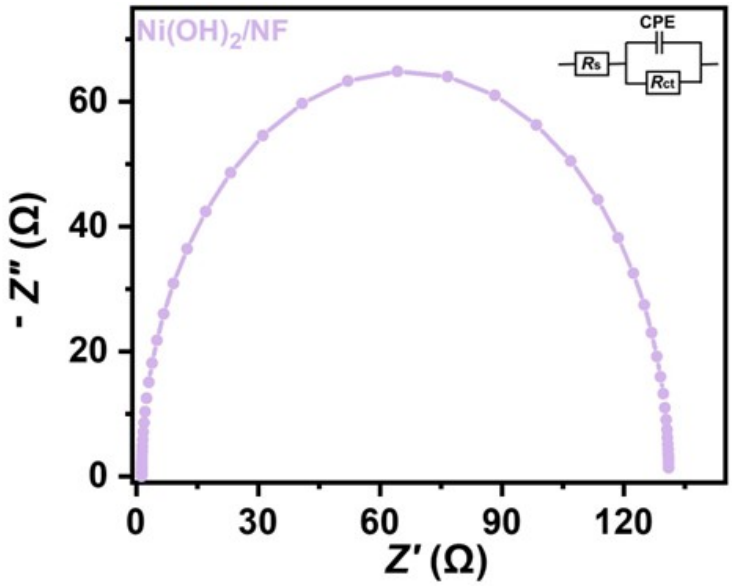

Figure S9. Nyquist plots of $Ni(OH)_2$/NF electrode at 0.5 V (vs. RHE) in 1 M KOH solution with 0.1 M 1,3-PDO.

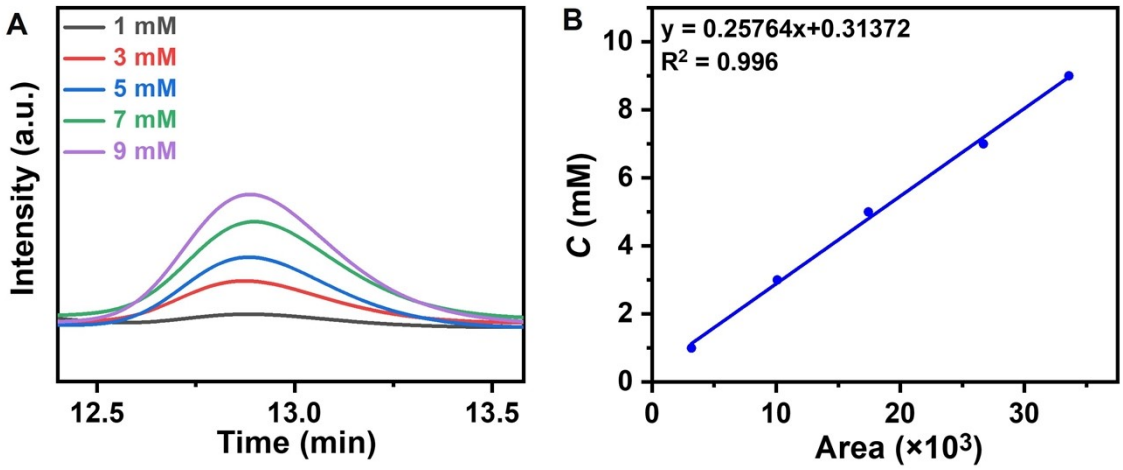

Figure S10. (A) Standard HPLC profiles for various concentrations of 3-hydroxypropionic acid; (B) Standard curve of 3-hydroxypropionic acid by correlating the concentration of 3-hydroxypropionic acid with corresponding peak area.

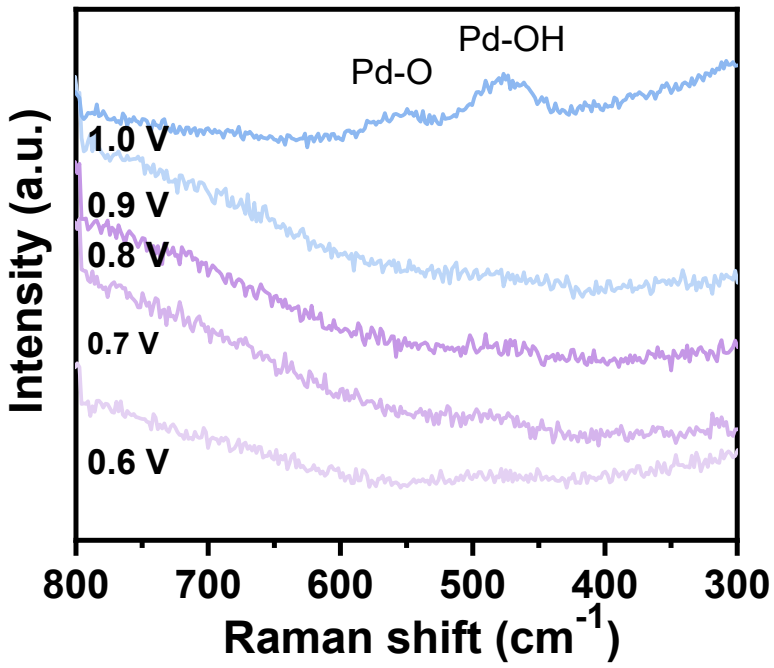

Figure S11. In situ Raman spectra of Pd−Ni(OH)$_2$/NF collected in 1 M KOH + 1 M EG with increasing potential.

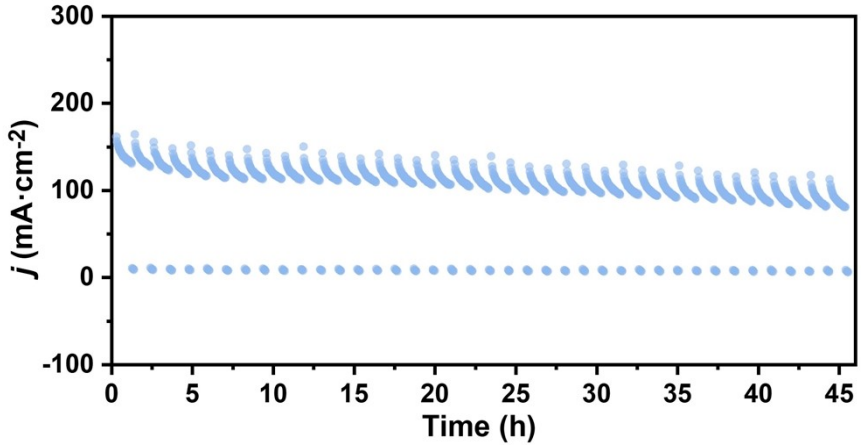

Figure S12. Stability tests of intermittent potential (IP) strategy for the Pd−$Ni(OH)_2$/NF electrode at 0.9 V (vs. RHE) for POR.

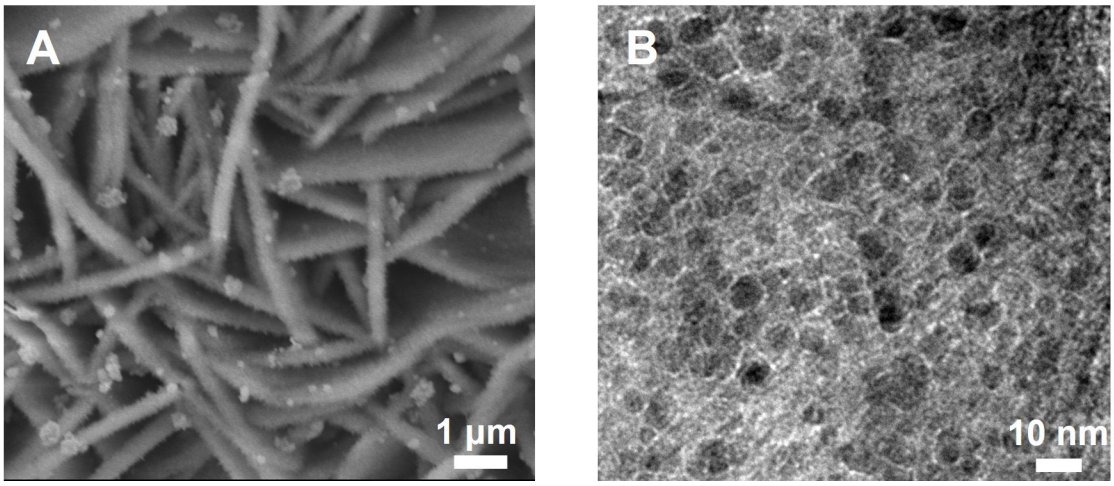

Figure S13. (A) SEM and (B) TEM images of Pd−$Ni(OH)_2$/NF electrode after POR electrolysis.

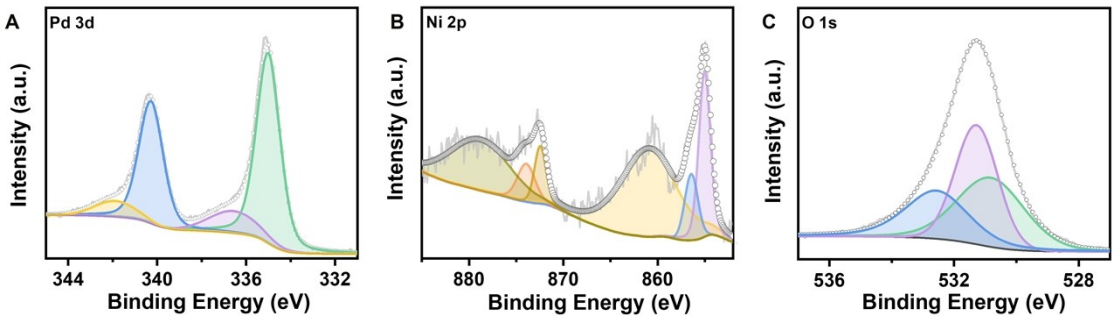

Figure S14. XPS spectra of (A) Pd 3d, (B) Ni 2p and (C) O 1s on the Pd−$Ni(OH)_2$/NF electrode after POR electrolysis.

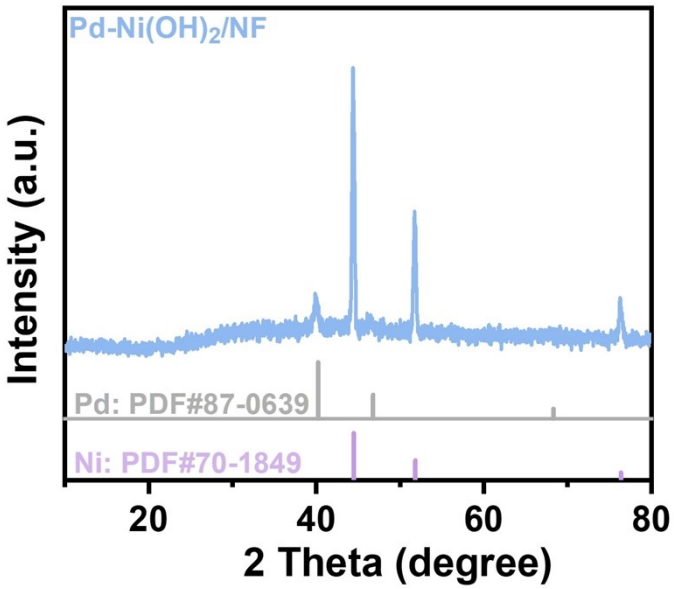

Figure S15. XRD pattern of the Pd−$Ni(OH)_2$/NF electrode after POR electrolysis.

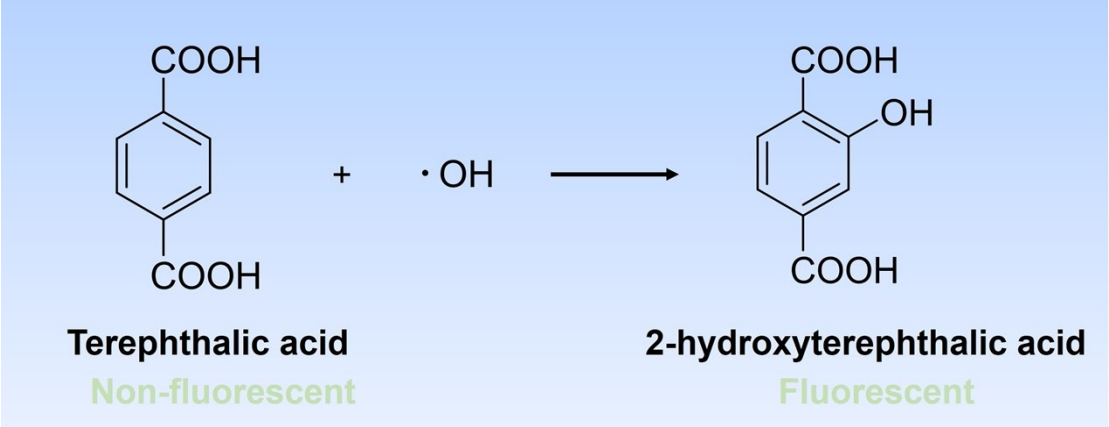

Figure S16. Reaction between the as-formed •OH and terephthalic acid.

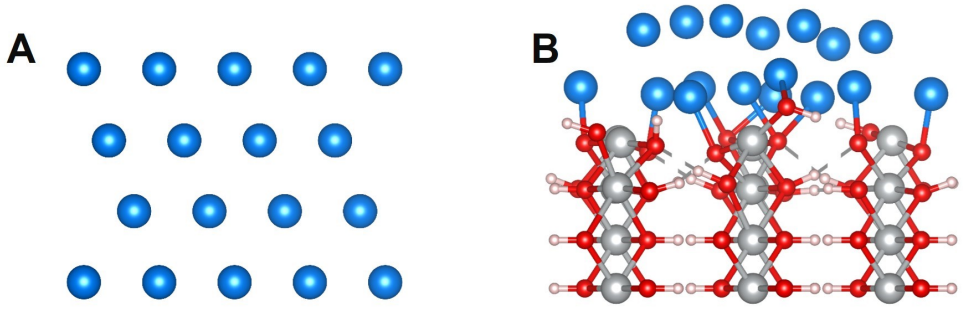

Figure S17. Theoretical models of Pd and Pd−$Ni(OH)_2$.

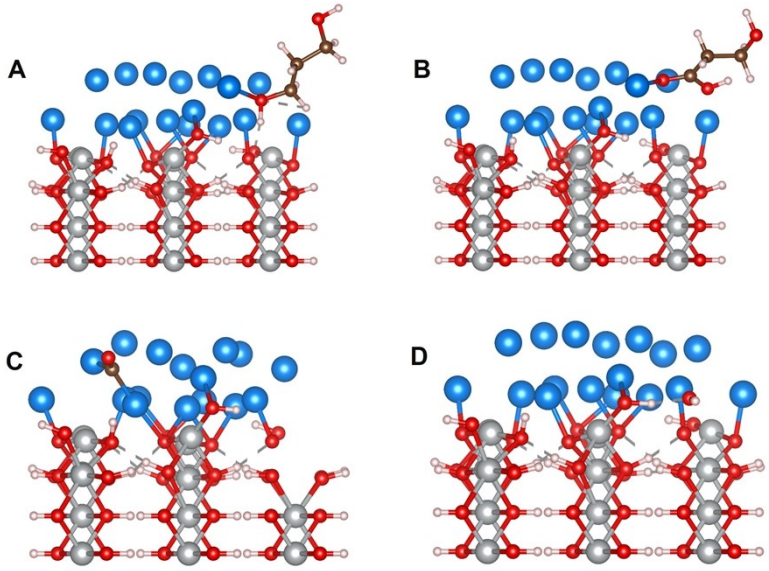

Figure S18. Adsorption model of (A) *1,3-PDO, (B) *3-HP, (C) *CO, and (D) *OH on the Pd−$Ni(OH)_2$ surface.

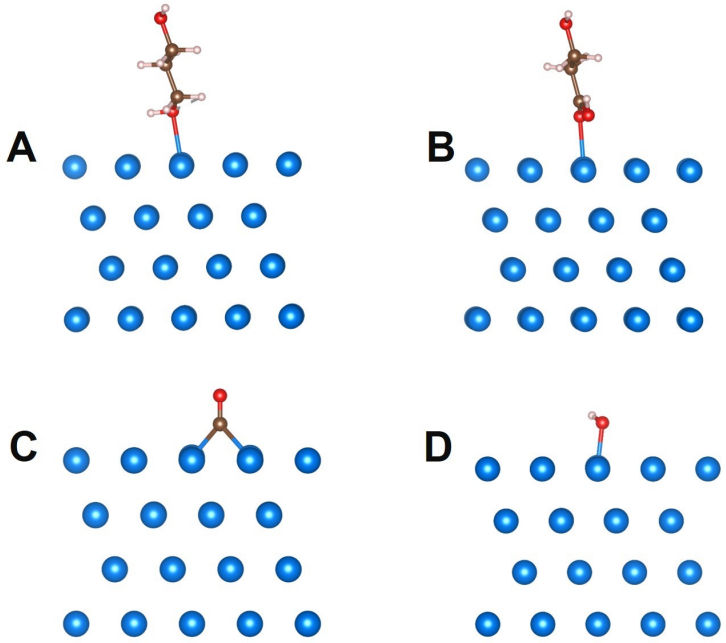

Figure S19. Adsorption model of (A) *1,3-PDO, (B) *3-HP, (C) *CO, and (D) *OH on the Pd surface.

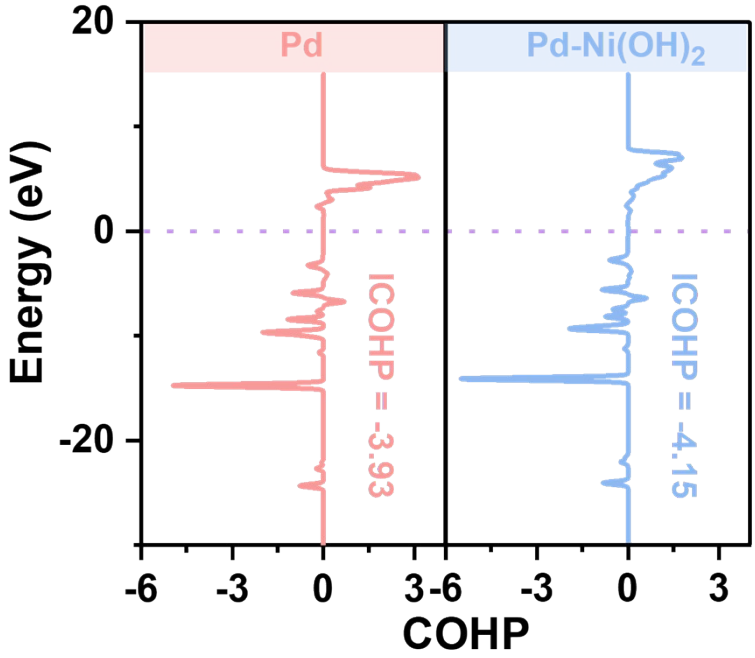

Figure S20. C–C bonds in *HOOC–CH_2CH_2OH adsorbed on Pd and Pd–$Ni(OH)_2$ surfaces.

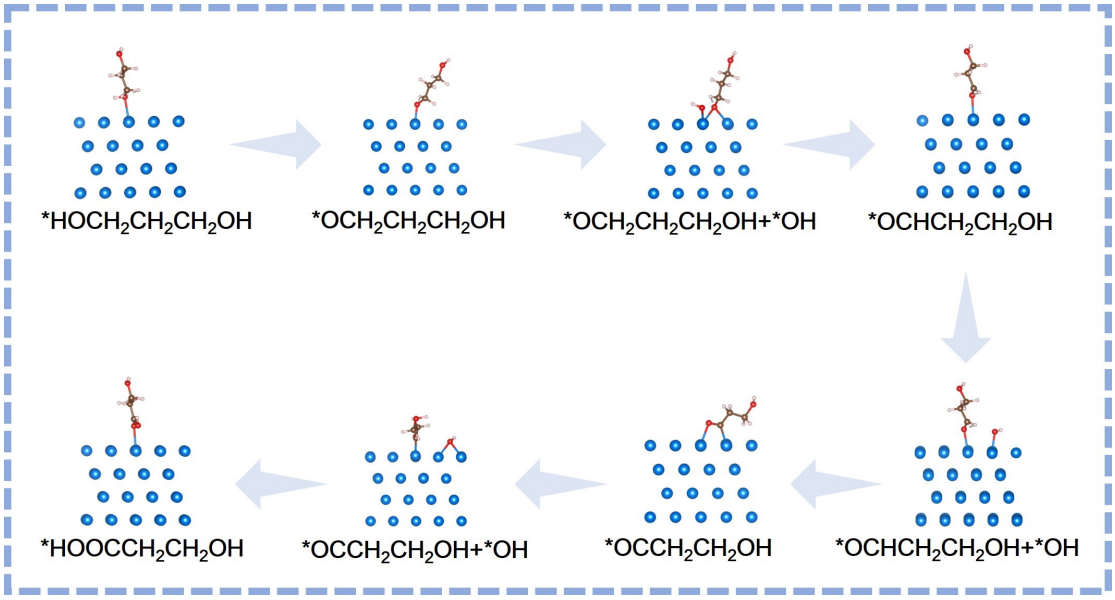

Figure S21. Optimized configurations of the 1,3-PDO oxidation process on Pd.

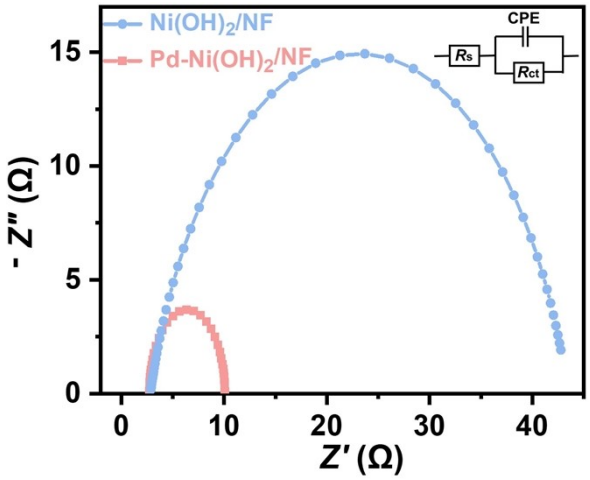

Figure S22. Nyquist plots of Pd−$Ni(OH)_2$/NF and $Ni(OH)_2$/NF electrodes at −0.1 V (vs. RHE) in 1 M KOH solution.

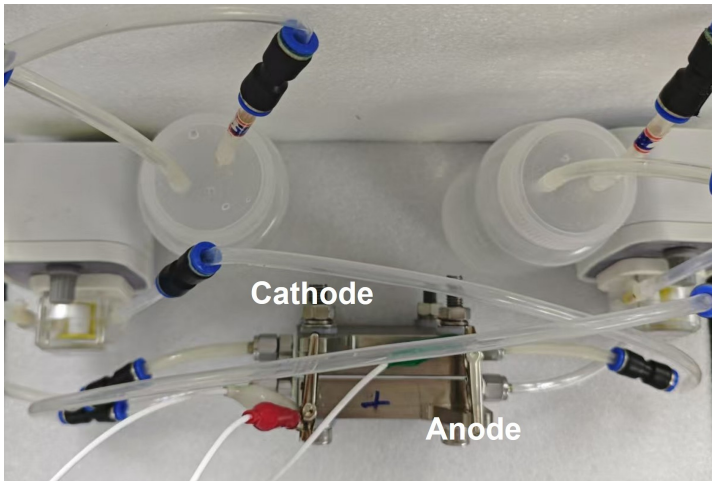

Figure S23. Photograph of the MEA system.

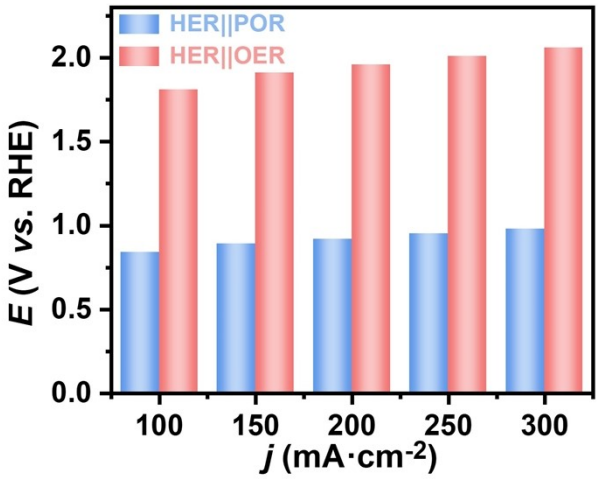

Figure S24. Comparisons of the potentials needed to achieve designated current densities for Pd−$Ni(OH)_2$/NF in 1.0 M KOH with and without 0.1 M 1,3-PDO.

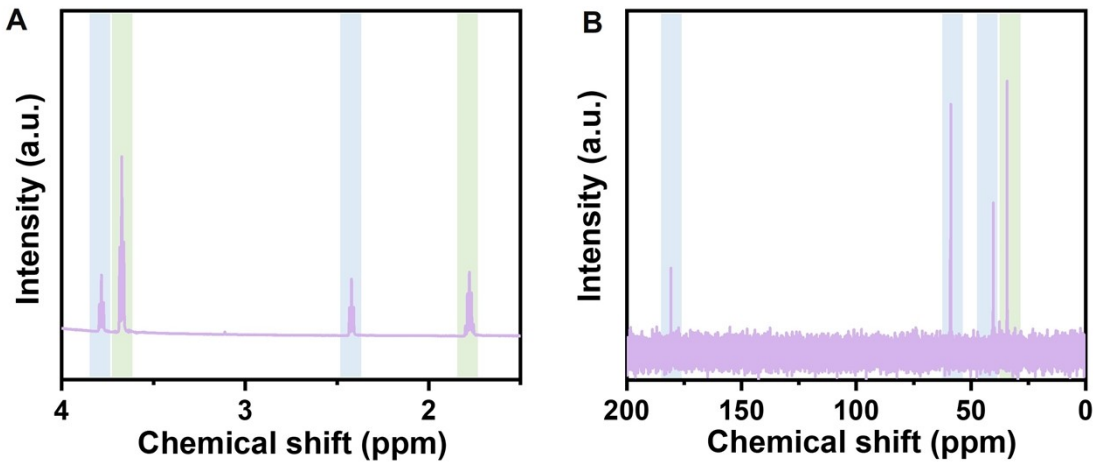

Figure S25. (A) ^{1}H NMR and (B) ^{13}C NMR spectra of the electrolyte after electrolysis.

Table S1. Comparison of HER performances of the Pd−$Ni(OH)_2$/NF electrode and other recently reported electrocatalysts in alkaline solution.

Electrocatalyst	*j* (mA cm^{-2})	η (mV)	Electrolyte	Reference
Pd−$Ni(OH)_2$/NF	10	50	1 M KOH	This work
	50	127	1 M KOH	This work
	100	168	1 M KOH	This work
Ni_2P-$Ni_{12}P_5$/NF	100	182	1 M KOH	[1]
RuO_2-WC NPs	10	58	1 M KOH	[2]
PtSA/Co_{AC}-O@ACTP	10	61	1 M KOH	[3]
Rh-MoS_2	10	67	1 M KOH	[4]
Pt NWs/SL-$Ni(OH)_2$	10	70	1 M KOH	[5]
Ni_5P_4 NPs	100	210	1 M KOH	[6]
Ni-S-Se/NF	10	98	1 M KOH	[7]

Supplementary references

1. Y. Xu, T. Liu, K. Shi, H. Yu, K. Deng, X. Wang, Z. Wang, L. Wang and H. Wang, *J. Mater. Chem. A*, 2022, **10**, 20365-20374.
2. S.-C. Sun, H. Jiang, Z.-Y. Chen, Q. Chen, M.-Y. Ma, L. Zhen, B. Song and C.-Y. Xu, *Angew. Chem. Int. Ed.*, 2022, **61**, e202202519.
3. J. Zhang, M. Wang, T. Wan, H. Shi, A. Lv, W. Xiao and S. Jiao, *Adv. Mater.*, 2022,

34, 2206960.

4. X. Meng, C. Ma, L. Jiang, R. Si, X. Meng, Y. Tu, L. Yu, X. Bao and D. Deng, *Angew. Chem. Int. Ed.*, 2020, **59**, 10502-10507.
5. H. Yin, S. Zhao, K. Zhao, A. Muqsit, H. Tang, L. Chang, H. Zhao, Y. Gao and Z. Tang, *Nat. Commun.*, 2015, **6**, 6430.
6. A. B. Laursen, K. R. Patraju, M. J. Whitaker, M. Retuerto, T. Sarkar, N. Yao, K. V. Ramanujachary, M. Greenblatt and G. C. Dismukes, *Energy Environ. Sci.*, 2015, **8**, 1027-1034.
7. N. Chen, Y.-X. Du, G. Zhang, W.-T. Lu and F.-F. Cao, *Nano Energ.*, 2021, **81**, 105605.